CHEMICAL ENGINEERING TRANSACTIONS
VOL. 70, 2018
A publication of AIDIC
The Italian Association of Chemical Engineering
Online at www.aidic.it/cet
Guest Editors: Timothy G. Walmsley, Petar S. Varbanov, Rongxin Su, Jiří J. Klemeš

ISBN 978-88-95608-67-9; **ISSN** 2283-9216
DOI: 10.3303/CET1870277

Synthesis of Colloidal Suspension Based on Porous Silica Nanospheres and Its CO_2 Absorption

Yudong Ding*, Xiaoqiang Li, Liheng Guo, Qiang Liao, Xun Zhu

Chongqing Univ., Key Laboratory of Low-grade Energy Utilization Technologies and Systems, Shazheng St.174, Shapingba Dist., Chongqing 400030, China
dingyudong@cqu.edu.cn

It is urgent to reduce CO_2 emissions for minimizing the consequences of the greenhouse effect and carbon capture material is one of the key factors for CO_2 capture technology. In this work, colloidal suspension were prepared as sorbents by dispersing porous silica nanospheres modified by polyethylenimine (PEI-PSNs) in dimethyaminoethoxyethanol (DMEE). Porous silica nanospheres (PSNs) synthesized via an emulsion method had high surface area (874.58 m^2/g) and uniform morphology. The absorption of CO_2 was studied over a wide range of CO_2 pressure (0-200 kPa), temperature (25-55 °C) and PEI-PSNs concentration (0-50 wt%). Compared to DMEE and PSNs/DMEE, PEI-PSNs/DMEE have much more CO_2 absorption capacity, resulting from that DMEE could improve reaction of amino and CO_2. It was also found that the absorption amount increased firstly and then decreased with PEI-PSNs concentration increasing and the maximum absorption capacity was 1.056 mmol/g at 30 wt% PEI-PSMs at 25 °C and 150 kPa. The regeneration efficiencies of the solutions at 80 °C were higher than 92 % in 5 absorption-desorption circles. The novel sorbents showed an advantage of a higher regeneration efficiency at relatively lower temperature and had great energy-saving potential.

1. Introduction

Carbon dioxide is the major contributor of greenhouse effect. With the rapid development of modern industrialization, more and more fossil fuels have been used for energy supply, which has caused CO_2 concentration in the atmosphere up to 408.35 ppm from 280 ppm in 1950s (NOAA, 2018). The increase of global greenhouse effect threatens economies, environments, and human health. Consequently, it is urgent to reduce CO_2 emissions for sustainable environment development. CO_2 capture and sequestration (CCS) (Balat et al., 2007), an attractive approach to reducing CO_2 emissions, has come into being and is expected to play a vital role in CO_2 emission mitigation in the foreseeable future.

Currently, various types of materials have been developed to capture CO_2 selectively, reversibly and economically. One of materials for industrial application is aqueous solution of monoethanolamine (Olajire et al., 2010). It has a remarkably fast apparent absorption rate, but the main problems are its high energy consumption due to solvent regeneration, corrosion and degradation. Another is solid adsorbents such as amine-silica composite (Cecilia et al., 2016) and other porous materials (Ding et al., 2015), which have been investigated by many scientific communities due to their right pore volume, surface area and selectivity to efficiently separate CO_2. However, industrial application technology with solid adsorbents is immature.

The colloidal suspension as sorbents in this work were prepared by suspending porous silica microspheres impregnated with amine in DMEE. This sorbents with the fluidty of liquid can be easily developed in a continuous process for industrial application. In addition, the liquid phase allows us to use advanced heat integrations to recover a large fraction of the heat. Moreover, the addition of DMEE acted as a proton acceptor can improve the reaction ability of loading amino with CO_2.

Please cite this article as: Ding Y., Li X., Guo L., Liao Q., Zhu X., 2018, Synthesis of colloidal suspension based on porous silica nanospheres and its co2 absorption , Chemical Engineering Transactions, 70, 1657-1662 DOI:10.3303/CET1870277

2. Experiment

2.1 Preparation of PEI-PSNs/DMEE

In a typical synthesis, ethanol (25 mL) and CTAB (2.6 g) were dissolved in water (64 mL) to form a transparent aqueous solution. Then, the ammonia (0.55mL, 28 wt%) was added into the aqueous mix solution mentioned above. After vigorous magnetic stirring for 30 min at 60 °C, TEOS (8 mL) was added within 30 min. Stirring was continued for 2 h and then the solution was centrifuged, rinsed with distilled water and dried in a vaccum oven at 60 °C overnight. Finally, the solid product was calcined in air at 550 °C with a heating rate of 1 °C/min and kept for 5 h to produce PSNs.
PSNs were functionalized by impregnation method with low molecular weight (600 MW) PEI. PEI was dissolved in methanol and the mix solution was stirred at room temperature. Then, PSNs were added. Subsequently, the solution was stirred for 10h at room temperature. The products were then dried in an oven at 60 °C for 5 h and dried again in an oven under vacuum at 50 °C for 10 h (Li et al., 2014). The material was named as PEI-PSNs. Finally, the novel sorbents were obtained by dispersing the desired amount of PEI-PSNs into DMEE, named as PEI-PSNs/DMEE.

2.2 Characterization of materials

Adsorption-desorption isotherms at 77 K were acquired in a Micromeritics ASAP 2010. A degasification step for 5 h at 423 K under vacuum for PSNs and 8 h at 393 K for PEI-PSNs was carried out before each isotherm.
Scanning electron microscopy (SEM) images were obtained using a Field emission scanning electron microscope (Tecnai G2 F20, American). The sample surfaces were coated with gold before the SEM measurements. Transmission electron microscopy (TEM) images were recorded with a transmission electron microscope (JEM 1200EX, Japan). The powdered samples for the TEM measurements were suspended in ethanol and then dropped onto the Cu grids with holey carbon films the isotherms.
Fourier-transform infrared spectroscopy (FTIR) analysis was performed using a Thermal NEXUS spectrometer (Thermo Scientific) and KBr was used to press to tablet; the resolution and scan frequency were 8 $cm^{-1}$and 32 min^{-1}, respectively. The spectra were recorded in the 4000–400 cm^{-1} region.
C, H and N elemental contents were determined using a FLASH 2000 CHNS/O elemental analyzer (Thermo Fisher). For each material, three parallel samples were used for analysis.

2.3 CO_2 absorption-desorption

The absorption performance of CO_2 was investigated with a dual-vessel absorption system shown in Figure 1. It mainly consisted of a gas reservoir, a vacuum pump, a stainless steel absorption vessel (20 mL) with a magnetic stirrer, a water bath, and a pressure sensor with an accuracy of 0.32 kPa in the experimental pressure range. The temperature of the water bath was controlled with an uncertainty of ±0.5 K.

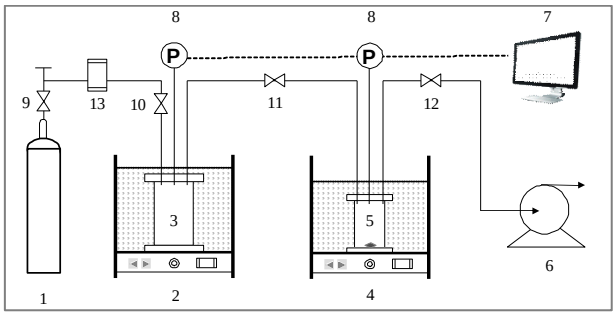

1: CO_2 cylinder
2, 4: magnetic stirrer and thermostatic water bath
3: CO_2 reservoir
5: CO_2 absorber
6: vacuum pump
7: data acquisition equipment
8: pressure sensor
9, 10, 11, 12: valve

Figure1: Schematic diagram of CO_2 absorption-desorption system

In a specific experiment, a known mass of PEI-PSNs/DMEE (about 5 g) solution was placed into the absorption vessel and the whole system was picked up the suction by vacuum pump. Then the gas reservoir (500 mL) was charged with CO_2 till the pressure reached the scheduled value. The valve 11 was turned on to let CO_2 be charged into the absorption vessel, in which the stirrer was started to enhance the dissolution of CO_2 in the absorbent. The pressure in the absorption vessel decreased with CO_2 absorption. It is supposed that equilibrium is reached after the pressure of the absorption is unchanged for 1 h. The absorption performance of CO_2 was investigated with a dual-vessel absorption system. According to the constant volume method for a dual-vessel absorption system, the amount of CO_2 absorbed can be calculated using the following Eq.(1):

$$n_{CO_2} = \frac{P_0 V_R - P(V_R + V_A - V_L)}{M_L RT} \quad (1)$$

Where V_R, V_A and V_L denote the volumes of storage vessel, absorption vessel and the absorbent, respectively. M_L represents mass the absorbent. P represents the saturated vapor pressure of liquid, and P_0 is the initial pressure in the storage vessel. M_L refers to the mass of sorbent.

3. Results and discussion

3.1 Characterization of materials

Figure 2(a) is the SEM and TEM images of PSNs. The SEM and TEM images clearly show that the morphology of PSNs synthesized via the emulsion approach are spherical. Besides, PSNs are nearly uniform and the average size of spheres about 120 nm. Noteworthy, the PSNs have excellent dispersibility and there is no aggregation among the nanospheres. In addition, porous channels of PSNs are observed from the high magnification TEM image.

The FTIR spectra of the PSNs and PEI-PSNs are shown in Figure 2(b). The bands of spectra (b)-1 located 426 cm^{-1}, 800 cm^{-1}, 1,099 cm^{-1} and 1,200 cm^{-1} were attributed to Si-O-Si vibrations. Besides, the weak absorption band at 564 cm^{-1} was ascribed to Si-O stretching vibrations and the band at 966 cm^{-1} resulted from Si-OH stretching vibrations. Moreover, the bands at 1,634 cm^{-1} together with between 3,750 cm^{-1} and 2,600 cm^{-1} were attributed to vibrations about water molecules that PSNs absorbed (Cecilia et al., 2012). Spectrum (b)-1 indicates that silica networks didn't be destroyed after calcination. On the other hand, spectrum (b)-2 shows all vibrations of silica networks. Furthermore, the bands at 1,310 cm^{-1} and 2,840 cm^{-1} were ascribed to C-N vibrations, and 2,950 cm^{-1} for CH_2 (Ji et al., 2012). Bands at 1,470 cm^{-1} and 1,575 cm^{-1} resulted from N-H (Nguyen et al., 2017). Finally, a wide band at 3,330 cm^{-1} was attributed to N-H. Thus, it can be seen that PEI have been loaded into PSNs successfully.

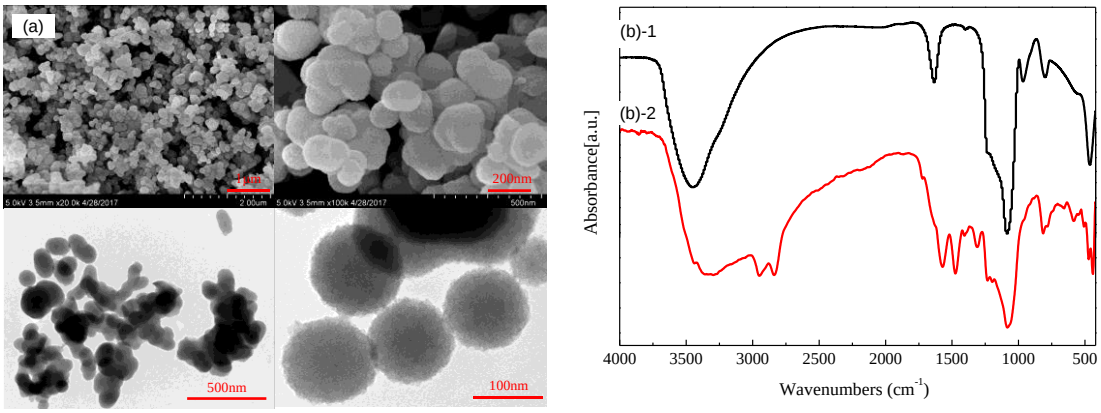

Figure 2: SEM and TEM images of PSNs (a); FTIR analysis of samples (b): PSNs (b)-1 and PEI-PSNs (b)-2.

Results of C, H, and N elemental analysis for PSNs and PEI-PSNs were listed in table 1. The table shows that C,H and N content of PEI-PSNs are higher than PSNs and N content of PSNs is 0, resulting from PSNs impregnated by PEI. Furthermore, PEI content based on elemental analysis was calculated. The PEI content was the result of the sum of C, H, and N content, which have deducted the C, H, and N content of plain silica. It was found that calculated value was nearly equal to experiment value.

Table 1: Element analysis of PSNs and PEI-PSNs

Sample	Elemental content (wt%)			N content (mmol/g)	PEI loading content (wt%)
	C	N	N		
PSNs	0.594	0.424	0	0	—
PEI-PSNs	33.248	8.422	18.877	1.348	59.529

N_2 adsorption-desorption isotherms of PSNs and PEI-PSNs, and the pore size distribution obtained by means of the density functional theory (DFT) model are represented in Figure 3. The nitrogen adsorption-desorption isotherms of PSNs shows type IV with a hysteresis loop in a range of P/P_0 (relative pressures) between 0.4 and

0.9, indicating that there are mesoporous pores in PSNs. The surface area of the sample was evaluated using BET method. Specific surface area and pore volume of PSNs are 874.58 m^2/g and 0.7397 m^3/g, respectively. However, specific surface area and pore volume of PEI-PSNs are only 15.9225 m^2/g and 0.0095 m^3/g, respectively. Such significant decrease of the textural properties of the grafted samples was due to the pore filling, which blocked the pores.

The detailed DFT pore size distribution illustrates that PSNs and PEI-PSNs shows narrow pore distribution with a peak value of 3.2 nm and 2.4 nm, respectively. In addition, it is observed that the average pore sizes of PSNs and PEI-PSNs are 2.74 nm and 1.98 nm, respectively.

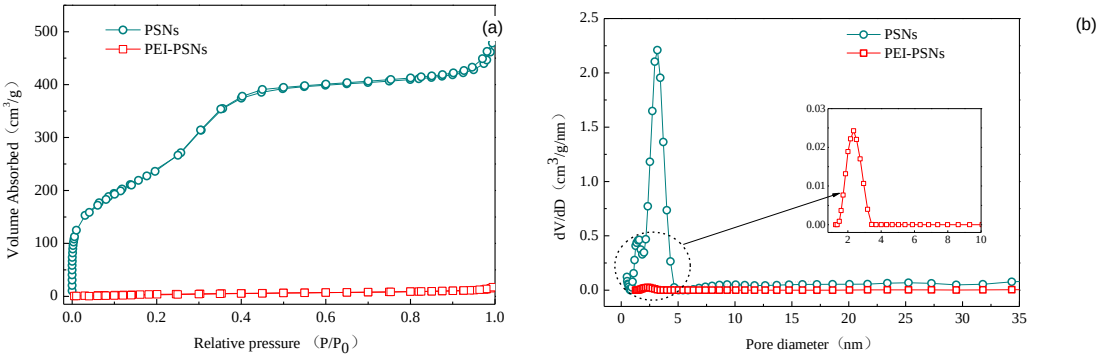

Figure 3: N_2 adsorption- desorption isotherms at 77K of the samples: PSNs and PEI-PSNs (a); pore size distribution of the raw samples: PSNs and PEI-PSNs (b).

3.2 CO_2 absorption

Here, novel sorbents consist of DMEE and PEI-PSNs. CO_2 absorption capacities of DMEE, PSNs/DMEE (10 wt%) and PEI-PSNs/DMEE (10 wt%) at 70 kPa and 25 °C were measured, as shown in Figure 4. It shows that CO_2 absorption capacity of DMEE, PSNs/DMEE and PEI-PSNs/DMEE are 0.1532 mmol/g, 0.1784 mmol/g and 0.4285 mmol/g, respectively. Compared to pure DMEE and PSNs/DMEE, PEI-PSNs/DMEE had much higher CO_2 absorption capacity, resulting from that DMEE could improve reaction of amino and CO_2 (Zhang et al., 2012).

Figure 4(b) shows the influence of absorption pressure on CO_2 absorption capacity of PEI-PSNs/DMEE (10 wt%). When pressure increases, CO_2 solubility coefficient of DMEE nearly shows a linear decline. However, CO_2 solubility coefficient of PEI-PSNs/DMEE (10 wt%) decreases sharply with pressure increase. The possible reason is that there are both physical absorption and chemical absorption in PEI-PSNs/DMEE. When pressure is over 150 kPa, CO_2 solubility coefficient of PEI-PSNs/DMEE (10 wt%) decreases very slowly. Thus, p=150 kPa was selected in the following experiment.

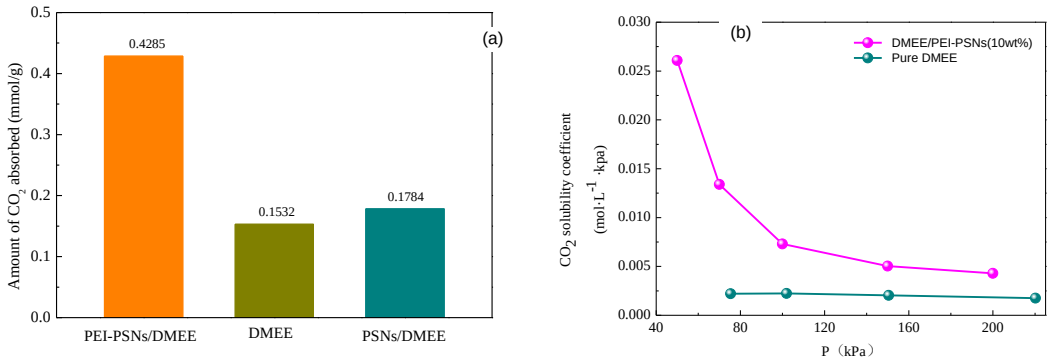

Figure 4: CO_2 absorption amount of DMEE, PSNs/DMEE and PEI-PSNs/DMEES at 70 kPa and 25 °C (a); CO_2 absorption solubility of DMEE and PEI-PSNs/DMEE at 25 °C (b).

Figure 5(a) and 5(b) show that CO_2 absorption amount and apparent absorption rate of PEI-PSNs/DMEE (10 wt%) at 150 kPa. Here apparent absorption rate is the average rate from beginning of CO_2 absorption to the time when CO_2 loading is up to 90 % saturation absorption amount according to the Damping-Film Theory

(Cadours et al., 2012), the relationship between the partial pressure of the gas and the absorption time can be described as：

$$\ln\{(P_1 - P_e)/(P - P_e)\} = ut \quad (2)$$

where P_1 and P_e represent the partial pressure of CO_2 at the beginning and at the equilibrium, respectively. P denotes the partial pressure at time t and u is the apparent absorption rate constant.
As shown in Figure(a), when the absorption temperature is between 25 °*C* and 55 °*C*, CO_2 absorption capacity decreases with the temperature. It can also be seen that the CO_2 apparent absorption rate increases with rising temperature. Furthermore, Table 2 shows the absorption capacity and apparent absorption rate in detail. It was found that the most absorption capacity of PEI-PSNs/DMEE (10 wt%) was 0.5656 mmol/g at 25 °*C* and the most apparent absorption rate was 0.0398 min^{-1} at 55 °*C*.

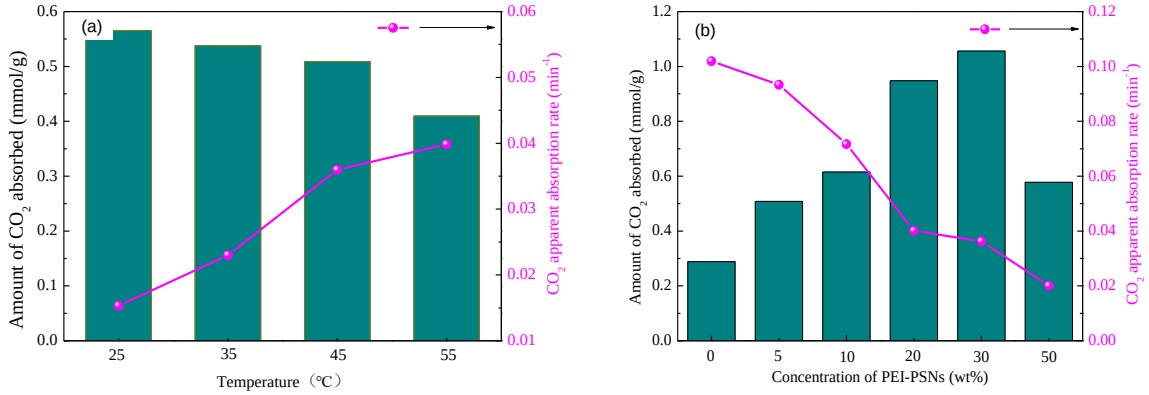

Figure 5: CO_2 absorption amount and apparent absorption rate of PEI-PSNs/DMEE at 150 kPa (a). CO_2 absorption amount and apparent absorption rate at 25 °C and 150 kPa (b).

Table 2: CO_2 absorption amount and apparent absorption rate of PEI-PSNs/DMEE at 150 kPa

Temperature(°C)	25	35	45	55
CO_2 absorption amount (mmol/g)	0.5656	0.5378	0.5090	0.4097
CO_2 apparent absorption rate (min^{-1})	0.0153	0.0230	0.0360	0.0398

As shown in Figure 5(b), when the concentration of PEI-PSNs in the novel sorbents is between 0 wt% and 30 wt%, the absorption capacity increases with the concentration of PEI-PSNs; When the concentration of PEI-PSNs is over 30 wt%, the absorption capacity decreases sharply. It can be seen from table 3 that 30 wt% PEI-PSNs is the best concentration in novel absorption and the absorption capacity of 30 wt% PEI-PSNs/DMEE can be up to 1.0561 mmol/g. On the other hand, in the range from 0 wt% to 50 wt% of PEI-PSNs concentration in novel sorbents, the apparent absorption rate decreases with rising concentration all the way. Since the viscosity of the solution will be increased with rising concentration, the higher viscosity is not beneficial for CO_2 diffusion in liquid.

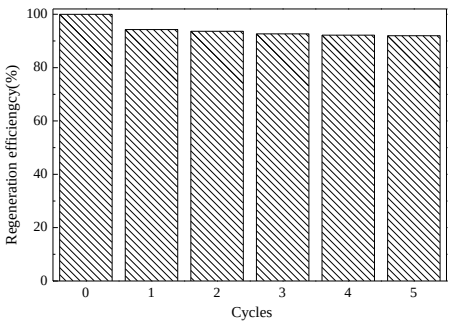

Figure 6: Regeneration efficiency of PEI-PSNs/DMEE at 80 °C under pure N_2.

Table 3: CO_2 absorption amount and apparent absorption rate of PEI-PSNs/DMEE at 25 °C and 150 kPa

PEI-PSNs concentration (wt%)	0	5	10	20	30	50
CO_2 absorption amount (mmol/g)	0.2887	0.5082	0.6150	0.9478	1.0561	0.5778
CO_2 apparent absorption rate (min^{-1})	0.1019	0.0933	0.0717	0.0401	0.0362	0.0201

3.3 CO_2 desorption

The results of the CO_2 absorption-desorption cycling analysis are presented in Figure 6. Novel sorbents could stand steady and its regeneration efficiency was still up to 92.0 % after 5 cycles at 80 °C. Meanwhile, the anhydrous formulation avoids the generation of water and therefore greatly saves the energy consumption during the regeneration process.

4. Conclusions

Porous silica nanospheres were synthesized via an emulsion method successfully. The obtained PSNs have high surface area (874.58 m^2/g) and excellent dispersibility, which can be used as good supporter of PEI. In addition, the novel sorbents was prepared by suspending PEI-PSNs in DMEE. Compared to PSNs/DMEE, PEI-PSNs/DMEE have much higher CO_2 absorption capacity. This is due to DMEE could improve reaction of amino and CO_2. CO_2 apparent absorption rate of PEI-PSNs/DMEE (10 wt%) increases but absorption capacity decreases with rising temperature. The most absorption capacity of PEI-PSNs/DMEE (10 wt%) is 0.5656 mmol/g at 25 °C and 150 kPa. The most apparent absorption rate is 0.0398 min^{-1} at 55 °C and 150 kPa. Concentration of PEI-PSNs in novel sorbents has a great influence on CO_2 apparent absorption rate and absorption capacity. The apparent absorption rate of PEI-PSNs/DMEE decreases all the way with rising concentration of PEI-PSNs concentration in novel sorbents. 30 wt% PEI-PSNs is the best concentration for CO_2 absorption and the absorption capacity can be up to 1.0561 mmol/g. Regeneration efficiency of PEI-PSNs/DMEE (10 wt%) was still up to 92.0 % after 5 cycles at 80 °C. The colloidal suspension show good cyclic stability and have great energy-saving potential.

Acknowledgments

We gratefully acknowledge the financial supports by National Science Foundation of China (No. 51576022) and National Science Foundation of China (No. 51276205).

References

Balat H., Öz C., 2007, Technical and economic aspects of carbon capture and storage - A review, Energy Exploration & Exploitation, 25 (5), 357-392.

Cadours R., Bouallou C., Gaunand A., Richon D., 1997, Kinetics of CO2 desorption from highly concentrated and CO2-Loaded methyldiethanolamine aqueous solutions in the range 312-383 K, Industrial & Engineering Chemistry Research, 36 (12), 87-95.

Cecilia J.A., Vilarrasa-García E., García-Sancho C., Saboya R.M.A., Azevedo D.C.S., Cavalcante Jr C.L., Rodríguez-Castellóna E., 2016, Functionalization of hollow silica microspheres by impregnation or grafted of amine groups for the CO2 capture, International Journal of Greenhouse Gas Control, 52, 344-356.

Ding Y.D., Song G., Zhu X., Chen R., Liao Q., 2015, Synthesizing MgO with a high specific surface for carbon dioxide adsorption, Rsc Advances, 5 (39), 30929-30935.

Ji C.C., Huang X., Li L., Xiao F.K., Zhao N., Wei W., 2016, Pentaethylenehexamine-Loaded hierarchically porous silica for CO_2adsorption. Materials, 9 (10), 835.

Li K., Jiang J.G., Yan F., Tian S.C., Chen X.J., 2014, The influence of polyethyleneimine type and molecular weight on the CO2 capture performance of PEI-nano silica adsorbents, Applied Energy, 136,750-755.

Nguyen Thi T.T., Tran T.V., Tran N.Q., Nguyen C.K., Nguyen D.H., 2017, Hierarchical self-assembly of heparin-PEG end-capped porous silica as a redox sensitive nanocarrier for doxorubicin delivery, Materials Science & Engineering C Materials for Biological Applications, 70 (Pt 2), 947.

Olajire A.A. 2010, CO2 capture and separation technologies for end-of-pipe applications - A review, Energy, 35 (6), 2610-2628.

US Department of Commerce, 2018, NOAA Research (www.esrl.noaa.gov/gmd/ccgg/trends/).

Zhang F., Gao K.X., Meng Y.N., Meng Y.N., Qi M., Geng J., Wu Y.T., 2016, Intensification of dimethyaminoethoxyethanol on CO2 absorption in ionic liquid of amino acid, International Journal of Greenhouse Gas Control, 51, 415-422.